Dynamical regimes of a paramagnetic particle circulating a magnetic bubble domain

Pietro Tierno,[1,2,*] Tom H. Johansen,[3] and Francesc Sagués[1,2]
[1]*Departament de Química Física, Universitat de Barcelona, Martí i Franquès 1, 08028 Barcelona, Spain*
[2]*Institut de Nanociència i Nanotecnologia (IN2UB), Universitat de Barcelona, Barcelona, Spain*
[3]*Department of Physics, University of Oslo, P.O. Box 1048, Blindern, Norway*
(Received 23 July 2009; published 17 November 2009)

We study the dynamics of a single paramagnetic colloidal particle dispersed in water and circulating around a cylindrical magnetic domain ("magnetic bubble") when driven by an external rotating magnetic field. We record the particle trajectories and measure its angular displacement by changing the strength, frequency, and ellipticity of the applied magnetic field and show that this simple system exhibits several interesting phenomena, from synchronous-asynchronous rotations, to localized oscillations. We complement the experimental results with numerical simulations which explore the dynamical regimes of the rotating particle.

DOI: 10.1103/PhysRevE.80.052401 PACS number(s): 82.70.Dd, 75.70.Kw, 05.45.Xt

I. INTRODUCTION

Colloidal particles can be used as a model system to study dissipative dynamics, since they are overdamped and their typical length and time scales are experimentally accessible. In this context there is an increasing interest in studying, both theoretically [1] and experimentally [2], the effect of confinement on the behavior of a system composed by a few such particles. Modern photolithography techniques allow the realization of complex topographic substrates used to confine microspheres into narrow channels [3], ratchetlike structures [4], or circular trenches [5]. However, such hard-wall confinement introduces a complex hydrodynamic coupling between the particles and the walls [6,7]. An alternative way to trap dielectric microspheres is to use optical methods such as fast scanning optical tweezers and holograghic techniques. A recent study by Roichman *et al.* [8] showed that already a simple system made by three Brownian particles diffusing along a light ring shows anomalous dynamical behavior. Theoretical simulations [9] on a similar system showed that hydrodynamic interactions between the diffusing particles lead to a limit cycle characterized by drafting of couples of particles.

Magnetic forces can be equivalently used to trap [10] and manipulate [11] paramagnetic particles without the use of topographic surfaces. In particular the periodic potential generated by a hexagonal array of cylindrical magnetic "bubble" domains in uniaxial ferrite garnet films have been used to transport [12], and sort [13] micron-size colloids. The magnetic bubbles are cylindrical ferromagnetic domains with uniform magnetization embedded in a film with opposite magnetization. Since the magnetic stray field of the film is maximum at the domain walls (DWs) corresponding to the bubbles perimeter, this allows to confine paramagnetic particles along a circle.

Here we study the dynamical regimes of a paramagnetic colloidal particle driven along the DW by an external rotating magnetic field. As control parameters we change the amplitude ($\hat{H}$), frequency (ω_H) and ellipticity (γ) of the applied field. The orientation of the ellipse with respect to the bubble lattice axes is kept fixed at $\pi/12$. At constant $\hat{H}$, we find three regimes of motion: the colloid at small ω_H follows synchronously the external field, at intermediate ω_H makes periodic backward and forward rotations and at high ω_H becomes localized over an arc of the bubble performing fast oscillations.

Changes in the field ellipticity unveil even new regimes which bridge the previous dynamical states. For particular values of the system parameters, we also observe intermittent switching between the localized state and the regime of asynchronous oscillations which results from the complex modulated magnetic potential.

II. EXPERIMENTAL PART

To create a magnetic bubble lattice we used a ferrite garnet film grown by liquid phase epitaxy on a gadolinium gallium garnet (GGG) substrate [14]. The magnetic film is characterized by a hexagonal lattice of ferromagnetic domains of radii $R=4.2$ μm and lattice constant $a=12.5$ μm, see Fig. 1(a). The film has saturation magnetization $M_s=7.6\times10^3$ A/m and thickness $h\sim5$ μm. We deposited above the film a diluted solution of paramagnetic colloidal particles (Dynabeads Myone) having radius $b=0.5$ μm and magnetic volume susceptibility $\chi=1.1$ [15]. A microscope image of

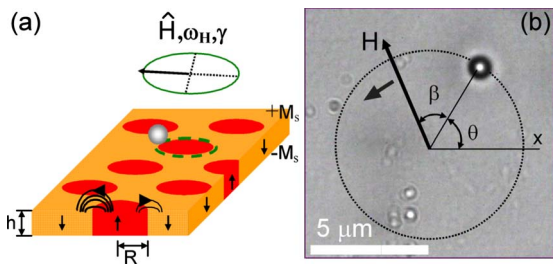

FIG. 1. (Color online) (a) Schematic of a garnet film with thickness h and saturation magnetization M_s embedding magnetic bubbles of radii R. Above the film we depict a paramagnetic particle subjected to a rotating magnetic field $\boldsymbol{H}$ with amplitude $\hat{H}$, frequency ω_H, and ellipticity γ. (b) Microscope image of one rotating particle with diameter 1 μm. The underlying magnetic bubble is not visible due to the absence of polarization elements in the optical system.

*ptierno@ub.edu

one such particle with its circular trajectory above a garnet film is shown in Fig. 1(b). The details on the experimental video microscopy and magnetic coil system has been given previously [16,17].

III. SIMULATION

The dynamics of the driven particle can be described by the overdamped equation,

$$\eta b f \frac{d\mathbf{r}}{dt} = -\nabla U(\mathbf{r},t), \tag{1}$$

where $\mathbf{r} \equiv (x,y)$, η is the water viscosity, f the drag coefficient which takes into account the proximity of the surface [18] ($f=56$) and $U(\boldsymbol{r},t) = -\frac{4}{3}\pi b^3 \mu_0 \chi \boldsymbol{H}_{tot}^2$ the magnetic potential. The total magnetic field acting over the particle is given by $\boldsymbol{H}_{tot} = \boldsymbol{H}_g + \boldsymbol{H}$, where $\boldsymbol{H}_g$ is the field due to a lattice of magnetic bubbles [19] and $\boldsymbol{H}$ denotes the external magnetic field, $\boldsymbol{H} = \hat{H}(\sqrt{1-\gamma}\sin\omega_H t, \sqrt{1+\gamma}\cos\omega_H t)$. $\boldsymbol{H}_g$ can be written following the superposition principle as a summation of the contribution due to individual magnetic bubbles [20]. For the magnetic stray field generated by one individual bubble at distance z from the film surface we used the expressions derived in the Appendix of Ref. [21].

IV. DYNAMICS

Let us consider a paramagnetic colloidal particle moving above a magnetic bubble domain. Since the magnetic stray field of the bubble has cylindrical symmetry, its perimeter is indeed a equipotential circle.

Application of a planar magnetic field breaks this symmetry and creates a gradient along the circle. When the field rotates, the particle lags behind the minimum and is forced to move. To characterize the regimes of motion we first fix $\gamma = 0$ (circular forcing) and vary ω_H and $\hat{H}$ of the applied magnetic field. Figure 2(a) shows the particle angular position θ versus time t for different frequencies at $\hat{H} = 1500$ A/m and time step $\Delta t = 0.0034$ s. When the frequency is low, θ increases linearly with time and the phase-lag angle β with the external field is constant, i.e., the dynamical regime is synchronous (SYN). Raising the frequency increases the dephasing angle with the field up to a first critical value, $\omega_1^c = 34.5$ s^{-1} where the motion becomes asynchronous (ASYN) and the particle starts to perform small backward oscillations each time β crosses π. Similar dynamical regimes has been previously observed and described in systems made by nonmagnetic particles dispersed in a ferrofluid [22] or for elongated paramagnetic ellipsoids [17]. Increasing further ω_H underscores a second critical frequency $\omega_2^c = 159.9$ s^{-1} above which the particle becomes localized (LOC). Now the field is too fast and the particle is not able to travel along the whole circle but describes small oscillations with an arc length decreasing with increasing ω_H.

In the ASYN regime the average angular velocity $\langle\omega\rangle = \lim_{T\to\infty}\frac{1}{T}\int_0^T \dot{\theta} dt$ decreases as ω_H increases and vanishes in the LOC regime. This is shown in Fig. 2(b) where $\langle\omega\rangle/\omega_H$ is plotted against ω_H for different values of $\hat{H}$. Here we combine the experimental data (open symbols) with the numerical results from the model (continuous lines) and observe good agreement. As expected from similar nonlinear rotating systems, increasing $\hat{H}$ shifts both ω_1^c and ω_2^c toward higher values. In the small inset of Fig. 2(b) we plot the critical frequencies ω_1^c and ω_2^c versus $\hat{H}$ and show the experimental data (closed symbols) together with the numerical results.

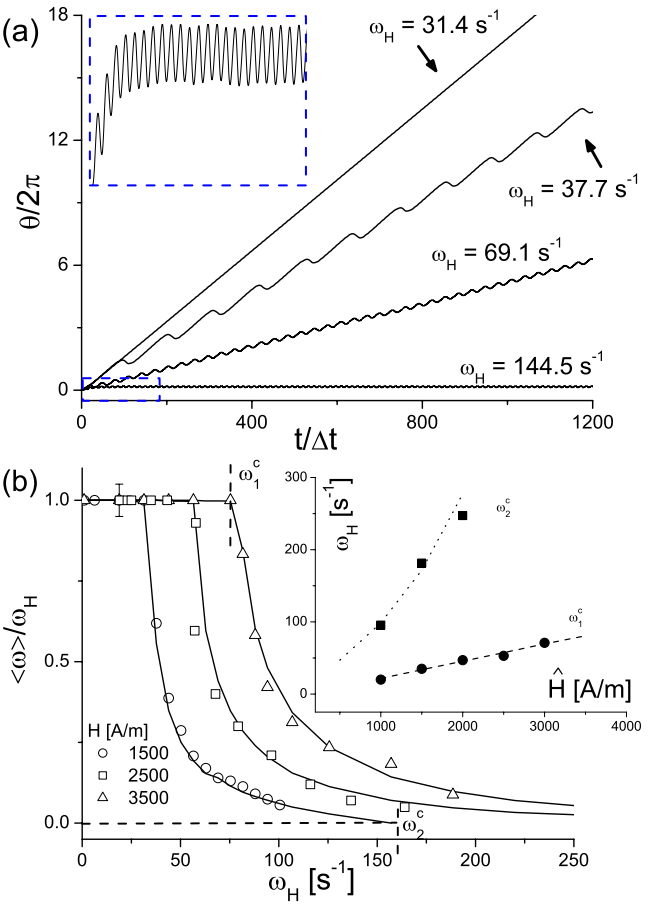

FIG. 2. (Color online) (a) Angular position $\theta/2\pi$ versus dimensionless time $t/\Delta t$ ($\Delta t = 0.0034$ s time step) of a paramagnetic particle at different field frequencies ω_H. The small inset enlarges a region of the localized oscillations for $\omega_H = 144.5$ s^{-1}. (b) Normalized angular velocity $\langle\omega\rangle/\omega_H$ versus frequency ω_H for different amplitudes $\hat{H}$ of the external field. The experimental data are shown as open symbols, the continuous lines are results from numerical simulations. Inset shows the critical frequencies ω_1^c (SYN→ASYN regimes), ω_2^c (ASYN→LOC regimes) versus field amplitude $\hat{H}$. The dashed (dotted) line refers to numerical results while the circles (squares) symbols represent experimental points for ω_1^c (ω_2^c).

Next we explore the effect of the field ellipticity on the particle dynamics. Figures 3(a) and 3(b) show how the angular position changes with increasing γ for $\hat{H} = 1500$ A/m. In Fig. 3(a) the particle is initially in the SYN regime, and remains in this mode for $\gamma \leq 0.6$, where the slope of the angular coordinate starts to decrease giving rise to the asynchronous oscillations.

Since this new dynamical regime which appears only for $\gamma > 0$ is a modulated version of the SYN one, we denote it as modulated (MD). In this regime of motion $\langle\omega\rangle$ decreases

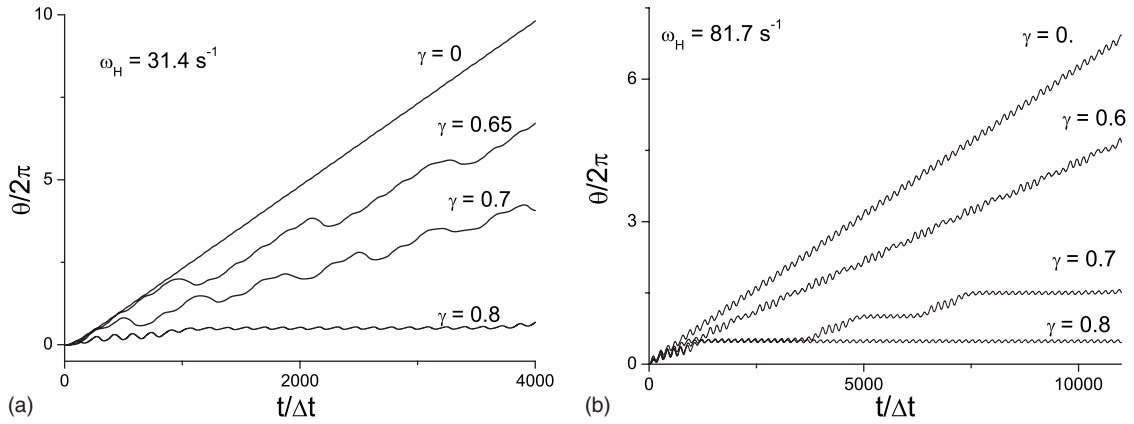

FIG. 3. Angular position $\theta/2\pi$ versus time $t/\Delta t$ of a circulating particle subjected to a rotating magnetic field with frequency ω_H $=31.4\ \mathrm{s}^{-1}$ (a) and $\omega_H=81.7\ \mathrm{s}^{-1}$ (b) for different field ellipticities γ. At $\gamma=0$ the particle dynamics is synchronous (a) and asynchronous (b) relative to the external field.

with increasing γ and vanishes for $\gamma>0.76$ where the particle passes to the LOC state. In Fig. 3(b) we consider the case of a particle initially in the ASYN regime (ω_H $=81.7\ \mathrm{s}^{-1}$). Increasing γ we observe a smooth transition to the MD regime and at large values of γ the appearance of an unstable regime (MD2), where the particle intermittently switches from being localized ($\langle\omega\rangle=0$) to perform asynchronous oscillations ($\langle\omega\rangle\neq 0$) along the circular path. The length τ of the localized regions (laminar phases) is not constant as found in the MD regime, but changes randomly as the trajectory develops in time. To better illustrate this behavior, we show in Fig. 4(a) a plot of $\theta/2\pi$ vs $t/\Delta t$ in this regime with the curve displaying a stair caselike structure. In Fig. 4(b) we show the distribution $P(\tau)$ of the laminar phases together with a power law fit. Both experimental data (filled circles) and numerical results (open squares) are shown as the scattered points. For short time intervals ($\tau<5$ s) we find that a power law scaling with an exponent $\alpha=2.2\pm0.1$ fits better the experimental points than an exponential (not shown), indicating anomalous dynamics [8,23]. Increasing slightly γ increases further the length of the laminar phase τ and the system could be expected to transit into chaos. However chaotic behavior is never observed in our system since by increasing the frequency the particle enters the LOC regime where it performs arc-length oscillations which are synchronized to the fast driving. We should point out that this regime is a consequence of the complex modulated magnetic landscape generated by the magnetic bubble and its six nearest neighbors. In fact running the simulation with only one magnetic bubble we were not able to observe the MD2 regime, but just another smooth transition from MD to LOC. Moreover we observe the MD2 regime only for particular orientations of the ellipse. If we call $\Delta\phi$ the angle difference between one of the three lattice main axes and the ellipse axis, the MD2 regime occurred only for $\Delta\phi$ $\in[0.02,0.05]2\pi$.

Figure 5 shows the phase diagram in the (ω_H,γ) plane illustrating the various dynamical regimes of the driven particle. The SYN regime covers a rectangular area with 0 $<\omega_H\leq 34.5\ \mathrm{s}^{-1}$ and $0<\gamma\leq 0.6$ while the ASYN a triangular one up to $\omega_H\gtrsim 160\ \mathrm{s}^{-1}$ in one vertex and $\gamma\sim 0.6$ on the other. The MD regime bridges both the SYN and ASYN dynamics toward the LOC state which covers also a triangular area and lasts for all $\omega_H\gtrsim 160\ \mathrm{s}^{-1}$ and $\gamma>0.8$. The MD2 regime was observed only in a small area between the MD and LOC and always for applied frequencies well inside the ASYN dynamics at $\gamma\neq 0$.

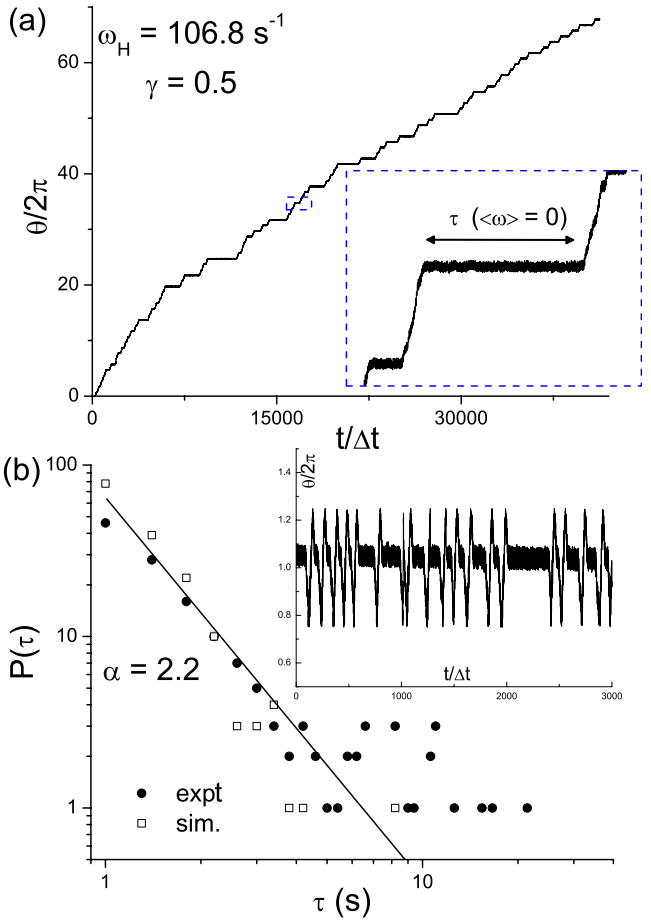

FIG. 4. (Color online) (a) $\theta/2\pi$ vs $t/\Delta t$ for $\omega_H=106.8\ \mathrm{s}^{-1}$ and $\gamma=0.5$. Small inset shows enlargement of the curve for 1600 $<t/\Delta<17\,000$. (b) Distribution $P(\tau)$ of the laminar lengths τ and scaling at short time. Small inset shows the $\theta/2\pi$ oscillations calculated by measuring $0<\theta<2\pi$.

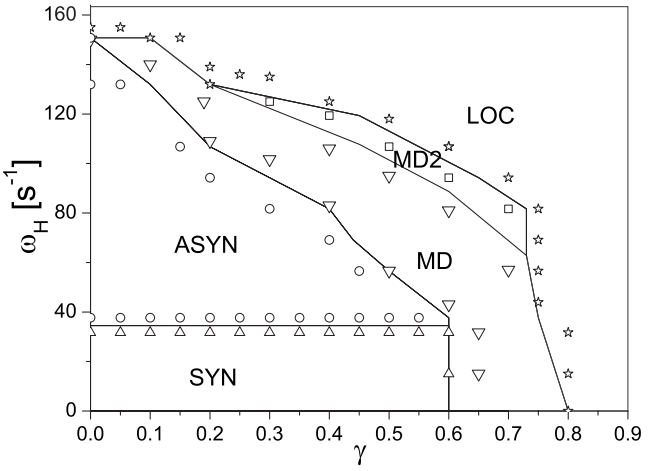

FIG. 5. Phase diagram in the (ω_H, γ) plane showing the various dynamical regimes denoted as: SYN=synchronous (up triangles), ASYN=asynchronous (circles), MD(1,2)=modulated (down triangles, squares), and LOC=localized (stars). The continuous lines follow from the simulation.

V. CONCLUSION

We studied experimentally and theoretically the overdamped dynamics of a micron-size paramagnetic colloidal particle circulating around a ferromagnetic bubble when subjected to an external rotating magnetic field. In a previous work [24] we used a similar system as a magnetic microstirrer device and measured the vorticity of the flow field generated by the rotating particles in water. However, here we used smaller paramagnetic particles which are closer to the DW and thus forced to perform larger circular trajectories. The larger particles used in [24] (2.8 μm) are less attracted from the DW and never show an asynchronous regime within the experimental parameters of Fig. 5. Their trajectory decrease in length as ω_H increases up to become localized in one point due to the large friction experienced during rotation at high ω_H. Thus at constant γ, increasing (decreasing) particle size should increase (decrease) the transition frequency from the SYN to ASYN regime up to a point in which only the SYN will appear in the phase diagram of Fig. 5. Conversely the LOC regime will increase (decrease) for smaller (larger) particles.

The controllable nonlinear motion of microscopic rotating particles could find application in microscale devices and flow mixing. For example interest has focused on the mixing properties of chains made by paramagnetic colloidal particles, unbound [25] or chemically linked [26]. Our system could in principle be equally used as a tool to achieve chaotic micromixing [27,28] by using a single rotating particle.

P.T. was supported by the program "Beatriu de Pinós" BP-B100167. P.T. and F.S. acknowledge financial support by MEC (Project No. FIS2006-03525) and DURSI (Grant No. 2005SGR00653). T.H.J. acknowledges The Research Council of Norway.

[1] I. V. Schweigert, V. A. Schweigert, and F. M. Peeters, Phys. Rev. Lett. **84**, 4381 (2000).
[2] R. Bubeck, C. Bechinger, S. Neser, and P. Leiderer, Phys. Rev. Lett. **82**, 3364 (1999).
[3] A. Terray, J. Oakey, and D. W. M. Marr, Science **296**, 1841 (2002).
[4] C. Marquet, A. Buguin, L. Talini, and P. Silberzan, Phys. Rev. Lett. **88**, 168301 (2002).
[5] Q.-H. Wei, C. Bechinger, and P. Leiderer, Science **287**, 625 (2000).
[6] B. Cui, H. Diamant, and B. Lin, Phys. Rev. Lett. **89**, 188302 (2002).
[7] V. N. Michailidou, G. Petekidis, J. W. Swan, and J. F. Brady, Phys. Rev. Lett. **102**, 068302 (2009).
[8] Y. Roichman, D. G. Grier, and G. Zaslavsky, Phys. Rev. E **75**, 020401(R) (2007).
[9] M. Reichert and H. Stark, J. Phys.: Condens. Matter **16**, S4085 (2004).
[10] L. E. Helseth, T. H. Johansen, and T. M. Fischer, Phys. Rev. Lett. **91**, 208302 (2003).
[11] L. E. Helseth, T. H. Johansen, and T. M. Fischer, Phys. Rev. E **71**, 062402 (2005).
[12] P. Tierno, T. H. Johansen, and T. M. Fischer, Phys. Rev. Lett. **99**, 038303 (2007).
[13] P. Tierno, A. Soba, T. H. Johansen, and F. Saguès, Appl. Phys. Lett. **93**, 214102 (2008).
[14] L. E. Helseth, T. Backus, T. H. Johansen, and T. M. Fischer, Langmuir **21**, 7518 (2005).
[15] L. Clime, B. L. Drogoff, and T. Veres, IEEE Trans. Magn. **43**, 2929 (2007).
[16] P. Tierno, S. V. Reddy, J. Yuan, T. H. Johansen, and T. M. Fischer, J. Phys. Chem. B **111**, 13479 (2007).
[17] P. Tierno, J. Claret, F. Sagues, and A. Cebers, Phys. Rev. E **79**, 021501 (2009).
[18] M. E. O'Neil, Mathematika **11**, 67 (1964).
[19] For computational speed purpose we consider only the effect of one magnetic bubble plus its six nearest neighbors. We observe that adding more magnetic bubbles to the system has no significant effect to the particle dynamics.
[20] A. Soba, P. Tierno, T. M. Fischer, and F. Saguès, Phys. Rev. E **77**, 060401(R) (2008).
[21] Y. S. Lin and P. J. Grundy, J. Appl. Phys. **45**, 4084 (1974).
[22] G. Helgesen, P. Pieranski, and A. T. Skjeltorp, Phys. Rev. A **42**, 7271 (1990).
[23] G. M. Zaslavsky, Phys. Rep. **371**, 461 (2002).
[24] P. Tierno, T. H. Johansen, and T. M. Fischer, J. Phys. Chem. B **111**, 3077 (2007).
[25] T. Roy, A. Sinha, S. Chakraborty, R. Ganguly, and I. K. Pu, Phys. Fluids **21**, 027101 (2009).
[26] S. L. Biswal and A. P. Gast, Anal. Chem. **76**, 6448 (2004).
[27] R. Calhoun, A. Yadav, P. Phelan, A. Vuppu, A. Garcia, and M. Hayes, Lab Chip **6**, 247 (2006).
[28] T. G. Kang, M. A. Hulsen, P. D. Anderson, J. M. J. den Toonder, and H. E. H. Meijer, Phys. Rev. E **76**, 066303 (2007).